

# Synthesis and Properties of Nanosilica-Reinforced Polyurethane for Grouting

X. J. Xiang,<sup>1</sup> J. W. Qian,<sup>1</sup> W. Y. Yang,<sup>1</sup> M. H. Fang,<sup>2</sup> X. Q. Qian<sup>2</sup>

<sup>1</sup>Department of Polymer Science and Engineering, Zhejiang University, Hangzhou 310027, China

<sup>2</sup>Department of Civil Engineering, Zhejiang University, Hangzhou 310027, China

Received 15 September 2004; accepted 24 June 2005

DOI 10.1002/app.23306

Published online 8 March 2006 in Wiley InterScience (www.interscience.wiley.com).

**ABSTRACT:** A polyurethane/nanosilica (PU/SiO<sub>2</sub>) hybrid for grouting was prepared in a two-step polymerization using poly(propylene glycol) diols as the soft segment, toluene 2,4-diisocyanate (TDI) as the diisocyanate, 3,3'-dichloro-4,4'-diaminodiphenylmethane (MOCA) as the chain extender, and acetone as the solvent. The size and dispersion of nanosilica, the molecular structure, mechanical properties, rheological behavior, thermal performance, and the UV absorbance characteristic of the PU/SiO<sub>2</sub> hybrid were investigated by transmission electron microscopy (TEM), FTIR, mechanical tests, viscometry, thermogravimetric analysis (TGA), differential scanning calorimetry (DSC), and UV

spectroscopy. Nanosilica dispersed homogeneously in the PU matrix. The maximum values of mechanical properties such as tensile strength, elongation break, and adhesive strength showed an addition of nanosilica of about 2 wt %. Resistance to both high and low temperatures was better than with PU. And the UV absorbance of the PU/SiO<sub>2</sub> hybrid increased in the range of 290–330 nm with increasing nanosilica content. © 2006 Wiley Periodicals, Inc. *J Appl Polym Sci* 100: 4333–4337, 2006

**Key words:** polyurethanes; silicas; nanocomposites; mechanical properties

## INTRODUCTION

It is well known that chemical grouting, which is an effective means of sealing water, stabilizing ground, and repairing cracks, is widely used in civil and mining engineering.<sup>1–2</sup> Conventional grouting materials such as bitumen and modified bitumen still possess a partial market share. However, with economic development and the development of construction, bituminous materials cannot meet the demands of applications because of its fatal drawbacks. In winter they are prone to chapping, and in summer they flow. Over the last 3 decades, interest in chemical grouting materials has been steadily increasing.<sup>3–7</sup> Among the synthesized polymer materials, PU occupies the most important position because it has excellent abrasion resistance and displays properties of both plastics and elastomers.<sup>8–10</sup>

Generally speaking, PU grouts can be divided into hydrophilic PU, hydrophobic PU, and elastomeric PU, depending on their reaction with water and their elongation.<sup>11</sup>

According to polymerization techniques, PU grouts can be synthesized by a variety of methods.<sup>12</sup> One-step polymerization is usually used to stop the flow of water, which results in a more random block polymer and a

reaction that is difficult to control. In contrast, two-step polymerization is used in the preparation of elastomeric PU grouts, a reaction that is easy to control.

As described above, there have been various studies of PU grouts; however, very few are currently available in the published literature on PU/SiO<sub>2</sub> hybrids for grouting. In our previous work, we prepared a pure PU grout by two-step polymerization.<sup>13</sup> In the present study, a PU/SiO<sub>2</sub> hybrid for grouting was synthesized, and some properties such as mechanical, rheological, and thermal properties were examined.

## EXPERIMENTAL

### Materials

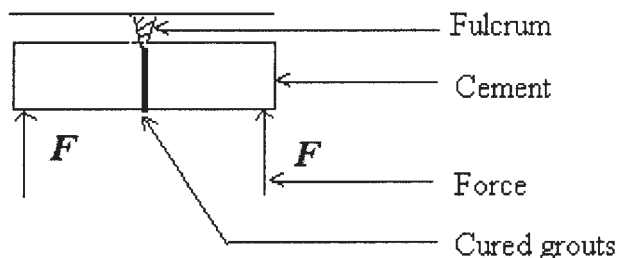
The reagents used in this study were nanosilica with a particle diameter of 10 nm and a surface area of 600 mm<sup>2</sup>/g, obtained from Haitai Nanomaterial Co. Ltd. (Nanjing, China); toluene 2,4-diisocyanate (TDI, L.R.); and poly(propylene glycol) diols (PPG) with a number-average molecular weight of 1000, obtained from Hangzhou Electronical Group Auxiliary Chemical Co., Ltd. (Hangzhou, China), triethanolamine (TEA, A.R.), acetone (A.R.), and 3,3'-dichloro-4,4'-diaminodiphenylmethane (MOCA) chain extender, obtained from Hangzhou Congsun Chemical Co., Ltd. (Hangzhou, China).

### Preparation of PU/SiO<sub>2</sub> hybrid

Polymerization was carried out in a two-step process. PPG was heated to 120°C under vacuum for 2 h to

Correspondence to: J. W. Qian (qianjw@zju.edu.cn).

Contract grant sponsor: NNSFC; contract grant number: 50173034.



Scheme 1 Sketch of antifold intensity test.

remove water and gases dissolved before use. Different amounts of nanosilica (1, 2, 3 wt %) were mixed with the treated PPG. TDI was introduced into a three-necked flask and heated to 80°C with mechanical stirring. Then the PPG-containing nanosilica was added with stirring for 2.5 h at a continued temperature of 80°C to form a prepolymer. The prepolymer was degass fully *in vacuo* and then cooled to room temperature. Afterward, the chain extender dissolved in acetone was added slowly under mechanical stirring. After 10 min of the reaction, the grouts were cast into a stainless-steel mold and cured at room temperature.

### Characterization

FTIR spectra of PU grouts with and without nanosilica were obtained with a Bruker VECTOR 22 FTIR spectrometer using solution-cast films on KBr disks.

TEM images of the PU/SiO<sub>2</sub> hybrid were measured with a JEM-1200 EX (Japan) apparatus. The samples were midrotomed into slices about 50 nm thick.

Tensile tests were carried out according to GB528-1998. All the results are an average of at least five measurements.

Measurement of adhesive strength was carried out with an indirect method in which the adhesive

strength was replaced by the antifold intensity. An artificial fissure was cut into the middle of a cement samples 4 × 4 × 16 cm in size. Then the grout was coated on the surface of the fracture. After curing the cement samples were tested using a DKZ-500 electric antifold instrument. If the ruins occurred on the surface of the fracture, adhesive strength was obtained. All results are an average of at least three measurements. The sketch is shown in Scheme 1.

The density ( $\rho$ ) of the grouts was measured at 30°C by the density bottle method. Three parallel measurements were carried out for each sample.

The viscosity of the PU/SiO<sub>2</sub> grouts was measured by a falling-sphere viscometer at 30°C and calculated according to Stokes' law.<sup>14</sup>

$$\eta = \frac{d^2 g (\rho_{fb} - \rho_s)}{18v}$$

where  $g$  is the gravitational constant (cm/s<sup>2</sup>);  $d$  and  $v$  are the diameter (cm) and the velocity (cm/s), respectively, of the falling ball; and  $\rho_{fb}$  and  $\rho_p$  are the density (g/cm<sup>3</sup>) of the falling ball and the grout liquid, respectively.

The gel time of the PU/SiO<sub>2</sub> grout was also measured with a falling-sphere viscometer at 30°C. Gel time was defined as the time at which the glass ball stopped in the viscometer with the PU/SiO<sub>2</sub> grout.

Thermal stability of the PU/SiO<sub>2</sub> hybrid was examined with a Perkin Elmer Pyri 1 thermogravimetric analyzer (TGA) under a nitrogen-protective atmosphere. The temperature profile went from 60°C to 600°C at a heating rate of 20°C/min.

The differential scanning calorimetry (DSC) curves of the PU/SiO<sub>2</sub> hybrid was obtained with a Perkin Elmer PYris 1 DSC under a N<sub>2</sub> atmosphere at a heating rate of 20°C/min from -60°C to 150°C.

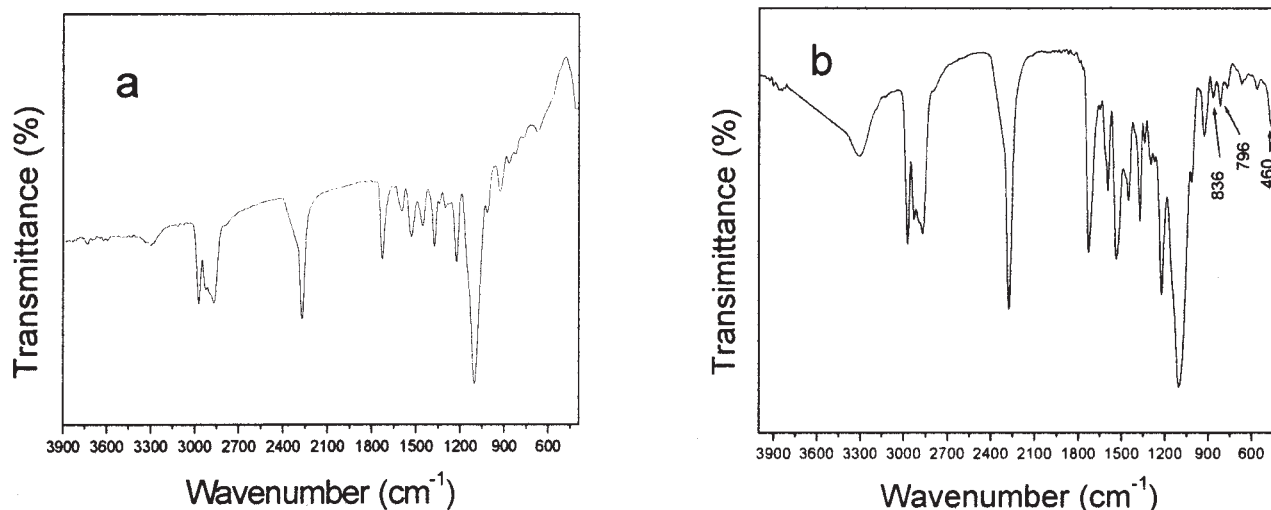


Figure 1 Typical IR spectra of samples: (a) pure PU grouts; (b) PU/SiO<sub>2</sub> grouts.

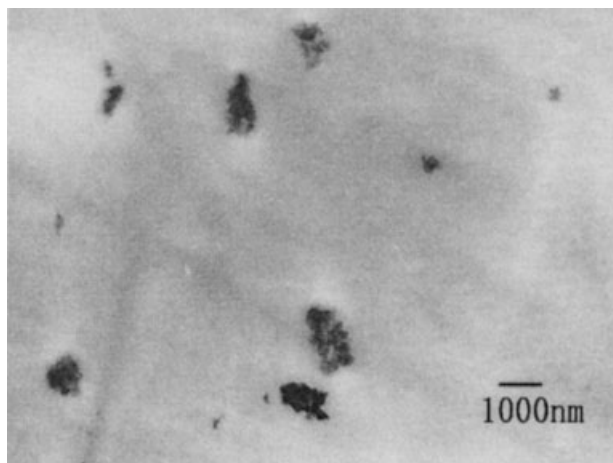


Figure 2 TEM micrograph of PU/SiO<sub>2</sub> hybrid.

The UV-vis spectra of the PU/SiO<sub>2</sub> hybrid were obtained by a CARY 100 Bio UV-visible spectrophotometer.

## RESULTS AND DISCUSSION

### Structure and morphology of hybrid

Figure 1 shows a comparison of both FTIR spectra for pure PU and PU/SiO<sub>2</sub> grouts. It can be seen in Figure 1(a) that the PU spectrum displays distinctive absorption bands at 3286, 2971, 2870, 2270, 1728, 1530, 1225, and 1106 cm<sup>-1</sup>. According to the characteristic peaks, C=O (1728 cm<sup>-1</sup>) and N-H (3286 and 1530 cm<sup>-1</sup>), the formation of the urethane group (—NHCOO—) was confirmed. It can also be seen from the spectrum of the PU/SiO<sub>2</sub> grout, shown in Figure 1(b), that most of the characteristic peaks, such as 3286, 2971, 2270, 1728, 1530, 1225, and 1106 cm<sup>-1</sup>, remained. However, three new absorption peaks were observed: at 796 and 460 cm<sup>-1</sup>, ascribed to the symmetrical stretch vibration and bend vibration of Si—O—Si, and at 836 cm<sup>-1</sup>, attributed to the absorption of Si—O—C. This clearly confirmed a chemical bond between the nanoparticles and the PU matrix.

A TEM micrograph of a typical PU/SiO<sub>2</sub> hybrid with a nanosilica content of 2 wt % is shown in Figure 2. It can be seen that the nanosilica particles dispersed homogeneously in the PU matrix.

### Mechanical properties

The mechanical properties of the PU/SiO<sub>2</sub> hybrid were obtained from stress-strain experiments and adhesive tests. The effects of nanosilica content on the tensile strength, elongation at break, and antifold intensity are shown in Figure 3. It can be seen that both the tensile strength and the elongation at break increased with increasing nanosilica content from 0% to 2% and then decreased as nanosilica content increased

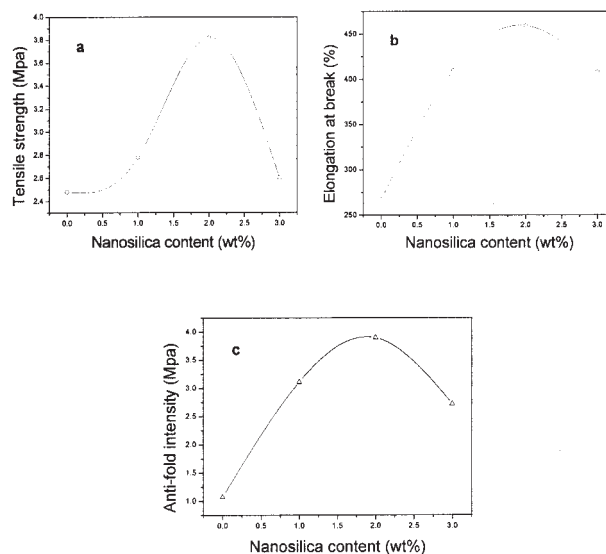


Figure 3 Effect of nanosilica content on mechanical properties of cured PU/SiO<sub>2</sub> grouts: (a) effect of nanosilica content on tensile strength, (b) effect of nanosilica content on elongation at break, (c) effect of nanosilica content on antifold intensity.

continuously. The maximum values of both tensile strength and elongation at break occurred at a nanosilica content of about 2 wt %. At the same time, the trend toward variation in antifold intensity versus nanosilica content was similar to that of the tensile strength and elongation at break. These results can be explained by the reaction between the NCO groups in TDI and both OH in polyol and nanosilica. This means that the chemical crosslink points formed because of the addition of nanosilica and hence improved the mechanical properties of the PU/SiO<sub>2</sub> hybrid. The higher antifold intensity was a result of the interaction of the hydrogen bonds between the PU/SiO<sub>2</sub> hybrid

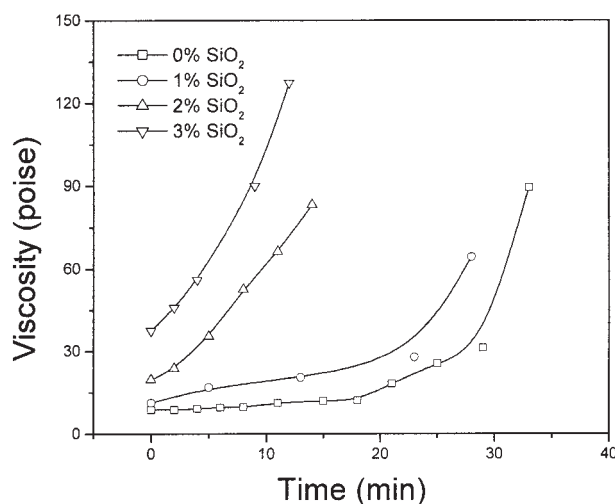
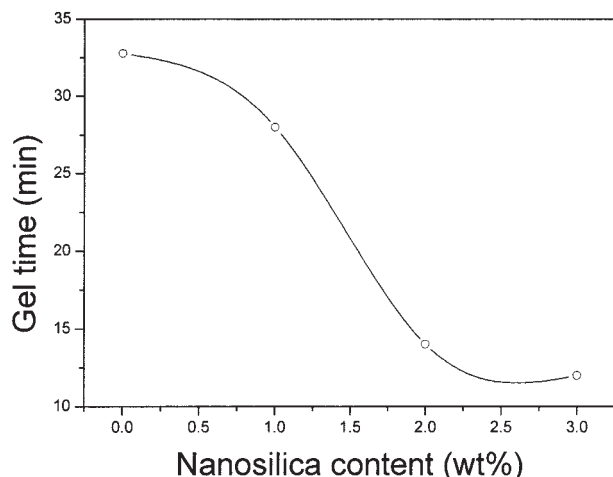


Figure 4 Effect of nanosilica content on viscosity of PU/SiO<sub>2</sub> grouts.



**Figure 5** Effect of nanosilica content in PU/SiO<sub>2</sub> grouts on gel time.

and the cement samples with OH groups and also of the better compatibility of the cement and the PU with inorganic nanosilica. After the maximum values were reached, the properties of the PU/SiO<sub>2</sub> hybrid decreased, probably because of the increasing aggregation of the nanosilica in the PU/SiO<sub>2</sub> hybrid.

### Rheological properties

Figure 4 shows the viscosity of the PU/SiO<sub>2</sub> grouts as a function of time in different nanosilica contents. A continuous increase in viscosity was observed with increasing nanosilica content, and the increase in viscosity, that is, the slope of each of curve, increased with increasing nanosilica content. After the last data point of each curve, the grout viscosity could not increase because of the falling glass ball being stopped in the viscometer with the grout. This supposed that

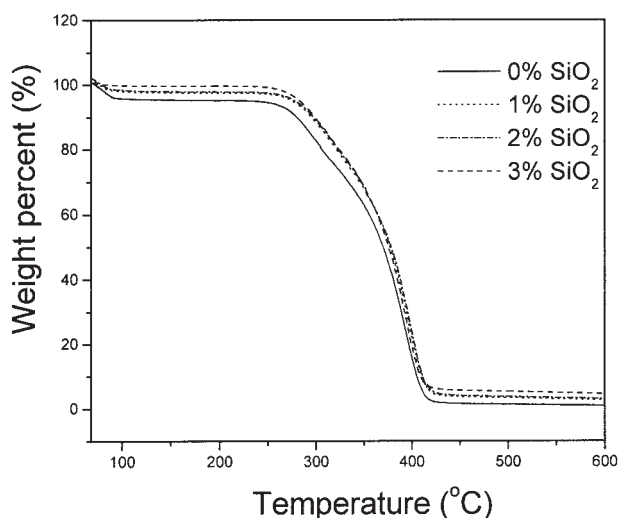


**Figure 6** TGA curves of cured PU/SiO<sub>2</sub> grouts.

**TABLE 1**  
Thermal Analysis Data of Cured PU/SiO<sub>2</sub> Grouts

Nanosilica content (%)	Initial weight loss temperature (°C)	$T_g$ (°C)
0	258.59	-12.605
1	266.08	-20.723
2	268.30	-20.834
3	273.61	-21.885

the gel had formed. The effect of nanosilica content on grout gel time is shown in Figure 5. It was found that gel time decreased with increasing nanosilica content because of more crosslinking between the silica and the polyurethane matrix.

### Thermal properties

The thermal stability of the PU/SiO<sub>2</sub> hybrid and PU were investigated by TGA. A typical TGA profile is shown in Figure 6, and the data are summarized in detail in the second column of Table I. It is evident that all the samples showed a one-stage decomposition, and the initial weight loss temperature (defined as a 5% weight loss temperature) of the PU/SiO<sub>2</sub> hybrid increased with increasing nanosilica content. This suggests that the thermal stability of the hybrid improved.

Figure 7 presents the DSC curves of PU/SiO<sub>2</sub> hybrids with different nanosilica contents, and Table I shows the glass-transition temperatures ( $T_g$ ) obtained. It can be clearly seen that each sample exhibited a single  $T_g$  for the soft segment and that the  $T_g$  decreased in the presence of nanosilica. A similar phenomenon for a polyimide-silica hybrid was reported by Morikawa et al.,<sup>16</sup> who considered the lower  $T_g$  to be a result of the low-molecular-weight silica, which was compatible with the polyimide matrix. Huang et

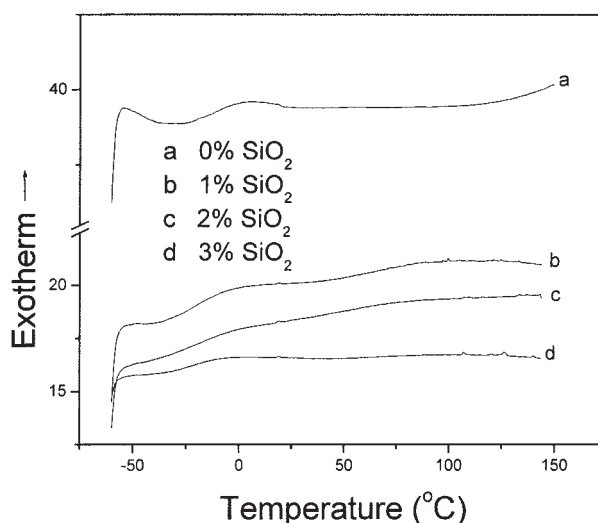


**Figure 7** DSC curves of cured PU/SiO<sub>2</sub> grouts.

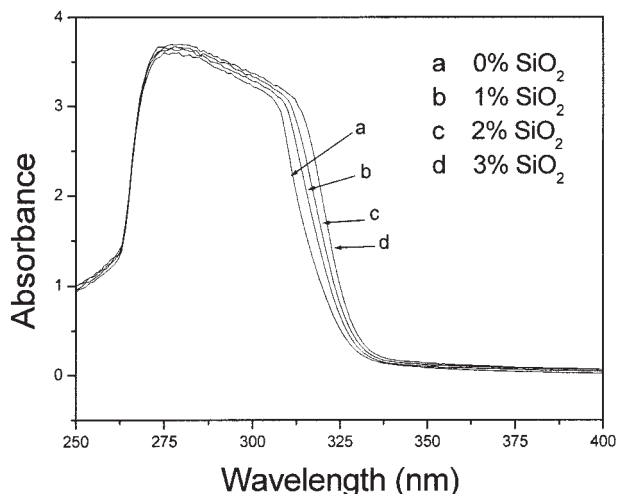


**Figure 8** UV-vis spectra of PU grouts with different nano-silica contents.

al.<sup>17</sup> demonstrated that the entanglements between chains could increase the  $T_g$  of the polymer. It is believed that the reduction of the  $T_g$  of the PU/SiO<sub>2</sub> hybrid in the present work probably can be attributed to the lesser entanglement between the polyol soft segments. This is because the regularity of the PU chain was disturbed partly because of the reaction between the NCO group of TDI and the OH group of the nanosilica, and the soft segment of the PU chain became comparatively more mobile.

### Optical property

The UV-vis absorbance of the PU/SiO<sub>2</sub> hybrid is shown in Figure 8, from which it can be seen that the absorbance at a wavelength of 290–330 nm increased with increasing nanosilica content. Yoshihito et al.<sup>18</sup> reported that the increasing UV absorbance of the polymer blend, that is, sequenced-ordered methacrylic acid copolymer and poly(4-vinylpyridine), was a result of the formation of hydrogen bonds between them. Therefore, it is believed that the increasing UV absorbance of the PU/SiO<sub>2</sub> hybrids also was a result of the formation of more hydrogen bonds in the composites. The increasing UV absorbance of the hybrid means that nanosilica could obstruct UV radiation; in other words, the weath-

erability of the PU/SiO<sub>2</sub> grouts was improved, which is good for their application on highways.

### CONCLUSIONS

A two-step polymerization was used to produce a two-component PU/SiO<sub>2</sub> hybrid for grouting. The nanosilica dispersed homogeneously and roughly on a nanometer scale in the PU matrix, and there were chemical bonds in the PU/SiO<sub>2</sub>. The introduction of nanosilica can greatly improve the mechanical properties of pure PU. When the nanosilica content was about 2 wt %, the tensile strength, elongation at break, and antifold intensity were at their maxima. With increasing nanosilica content, the PU grout showed increased viscosity and decreased gel time. The initial temperature of decomposition was higher in the PU/SiO<sub>2</sub> hybrid than in the pure PU. At a wavelength of 290–330 nm, the UV absorbance of the PU/SiO<sub>2</sub> hybrid increased with increasing nanosilica content.

### References

1. Smoak, W. G. *Concrete Int* 1991, 13, 33.
2. Darrag, A. A. *Tunn Undergr Sp Tech* 1999, 14, 319.
3. Vik, E. A.; Sverdrup, L.; Kelley, A., et al. *Tunn Undergr Sp Tech* 2000, 15, 369.
4. Weideborg, M.; Källqvist, T.; Sverdrup, L. E.; Vik, E. A. *Water Res* 2001, 35, 2645.
5. Eriksson, M. *Tunn Undergr Sp Tech* 2002, 17, 287.
6. Jones, M. *Tunnels Tunnelling* 1995, 27, 71.
7. Zelanko, J. C.; Karfakis, M. G. *Int J Rock Mech Min Sci* 1997, 34, 595.
8. Chen, A. T.; Wojcik, R. T. *Met Finishing* 2000, 98, 143.
9. Gogolewski *Colloid Polym Sci* 1989, 267, 757.
10. Garrett, J. T.; Runt, J.; Lin, J. S. *Macromolecules* 2000, 33, 6353.
11. Joyce, J. T. *Concrete Construction* 1992, 7, 551.
12. Mothe, C. G.; de Araujo, C. R. *Thermochimica Acta* 2000, 357–358, 321.
13. Xiang, X. J.; Qian, J. W.; Bai, Y. X., et al. *J Polym Mater* 2005, 22, 219–226.
14. Sperling, L. H. *Introduction to Physical Polymer Science*, 2nd ed.; Wiley & Sons: New York, 1992; p 493.
15. Hajji, P.; David, L.; Gerard, J. F.; et al. *J Polym Science, Part B: Polym Phys* 1999, 37, 3172.
16. Morikawa, A.; Iyoku, Y.; Kakimoto, M., et al. *Polym J* 1992, 24, 107.
17. Huang, D. H.; Yang, Y. M.; Zhuang, G. Q.; Li, B. Y. *Macromolecules* 2000, 33, 461.
18. Inai, Y.; Takenouchi, S.; Hirabayashi, T.; Yokota, K. *Polym J* 1996, 28, 365.